COMPDYN 2015
5th ECCOMAS Thematic Conference on
Computational Methods in Structural Dynamics and Earthquake Engineering
M. Papadrakakis, V. Papadopoulos, V. Plevris (eds.)
Crete Island, Greece, 25–27 May 2015

SLENDER LARGE-SCALE PARABOLIC TROUGHS USING SHAPE-OPTIMIZED HOLLOW STRUCTURES MADE OF HIGH-STRENGTH CONCRETE

Christoph Kämper[1], Janna Krummenacker[2], Patrick Forman[1], Peter Mark[1], Jürgen Schnell[2]

[1] Institute of Concrete Structures, Ruhr-University Bochum
Universitätsstrasse 150, 44780 Bochum, Germany
e-mail: christoph.kaemper@ruhr-uni-bochum.de

[2] Institute of Concrete Structures and Structural Engineering, Technical University Kaiserslautern
Paul-Ehrlich-Strasse, 67663 Kaiserslautern, Germany
janna.krummenacker@bauing.uni-kl.de

Keywords: Parabolic trough, high-strength concrete, hollow cross-section, optimization

Abstract. *Parabolic trough collectors focus insolation on receiver tubes to generate electricity in downstream steam cycles. Currently, commercially already established collector modules consist of spatial steel frameworks supporting mirror elements point-wise. The crucial disadvantage hereof is the separation between supporting and reflecting structure. To overcome this drawback, a yet small-scale but continuous concrete shell prototype, that combines both tasks, has been manufactured. It consists of a single thin-walled shell made from high-strength concrete with a thickness of 20 to 30 millimeters only. Tests have proven a considerable optical efficiency of the prototype developed in a cooperation of the universities of Bochum and Kaiserslautern in Germany.*

In line with current trends to reduce costs by economy of scale, an up-scaled structure based on the prototype, but having an aperture of 10 x 30 m and a hollow cross-section, is now aimed for. To account for the specific action effects on such structures, like wind loads and temperature, an initial numerical model has been set up. Employing topology optimization techniques delivers an optimally balanced model candidate with respect to mass and stiffness iteratively. Structural parts that require low densities only are identified and substituted by hollow shapes of simple geometry. That way, the total structure is subdivided into appropriate substructures according to the flux of inner forces along with a significant weight-reduction. Obviously, the emerging partial segments defined by the substructures have to be designed for stability. Accompanying experimental studies of micro-meshed reinforced high-strength concrete elements prove both general feasibility and also manufacturing.

1 INTRODUCTION

State-of-the-art for parabolic troughs is steel frameworks supporting curved mirror elements point-wise like in case of the EuroTrough module with an aperture of 5.77 x 12 m [1]. This kind of collectors has become the most mature technology in concentrating solar light during the last years. Today the worldwide installed power amounts to more than 2 GW. But, a disadvantage of these troughs has been claimed, too. Due to the point-wise supported mirror elements potential energy losses might arise, e.g. from wind-induced, deformation in between the boundary points. Recently, this drawback has been tackled in cooperative investigations of the two universities of Bochum and Kaiserslautern in Germany. A small-scale prototype made from concrete has been developed that merges support and reflection in a shell-like structure. To reflect solar light, a foil is glued plane on the concrete surface. Their small-scale prototype has an aperture of 2.205 x 3.20 m along with a thickness 2-3 cm only. However, it shows the general feasibility of highly accurate concrete collector modules with proven optical performance [2]. Extending these fundamental findings and following current trends to reduce costs by economy of scale, a parabolic trough module of 10 x 30 m is now aimed for. To realize these dimensions with concrete, structural weight must clearly be saved. The massive single-walled concrete shell is dissolved into a hollow structure. Employing topology optimization techniques the cross-section is re-designed claiming volume decrease and stiffness gains simultaneously. In an initial step before, the design space for topology optimization must be restricted with respect to stiffness, low deformation and the concrete's tensile strength pivotal for cracking. First results of this iterative form-finding process are presented in the remainder.

2 CONCEPTUAL DESIGN

Recently published conceptual designs of parabolic trough collector modules consist of thin-walled concrete shells made of high-strength concrete in which reflectors on the inner surface are adapted that do not contribute to structural bearing capacity [3, 4]. They concentrate on the concrete shell and do not comprise detailed analyses of the supports what might be necessary in a holistic optimization. Inspired by the EuroTrough module a small-scale prototype with homogenous cross-section has been manufactured with wall thicknesses of 3 cm at vertex and 2 cm at the free edge [2]. In case of large-scale parabolic troughs similar low wall-thicknesses can be achieved dissolving a homogeneous concrete cross-section into an inhomogeneous hollow one. That way, significant portions of self-weight are saved whereby the adaptive inner lever arm of forces, the distance between compressive and tensile stress resultants in concrete, grants high stiffness. Following the concept of non-cracked concrete, the size of the inner lever arm is restricted by allowable tensile stresses due to concrete's tensile strength with respect to intended wall-thicknesses. Additionally, low deformations must be met to obtain high surface accuracy and total efficiency of the collector. An inhomogeneous cross-section shall be obtained by adjusted hollow shapes describing the inner geometry especially the position of vertical struts. Initial geometry and material properties of an envisaged large-scale trough module are presented in Fig. 1 and Table 1.

Young's modulus	47 593 N/mm²
Bending tensile strength	15.1 N/mm²
Cylindrical compressive strength	109.1 N/mm²
Density of hardened concrete	2524 kg/m³

Table 1: Material properties of hardened Nanodur® concrete (mean values, determined at TU Kaiserslautern).

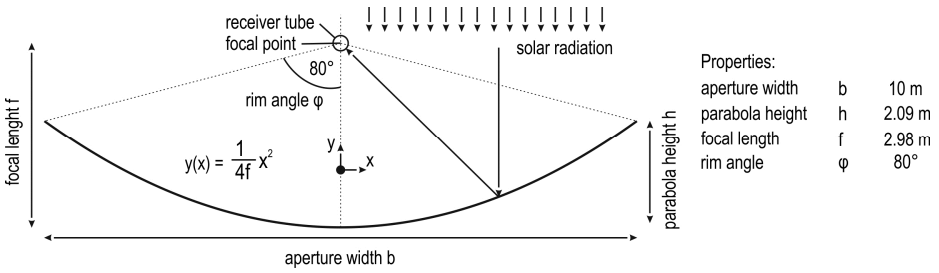

Figure 1: Sketch and dimensions of a large-scale parabolic trough.

While the inner shape of the collector is required to be smooth and can be best described by a general parabolic function, the exterior shape is optional. This gives the opportunity to search for an optimum shape. Eq. 1 relates the focal length f of 2.98 m to a rim angle φ = 80 and an aperture width b = 10 m with respect to a computational module model.

$$y(x)=\frac{1}{4f}x^2 \tag{1}$$

To investigate the exterior contour on bottom side, the cross-section has been modelled as a cantilever beam. Its length is half the aperture width due to symmetry. Further, the so called design space (cf. Fig. 2, top left) is defined by six design variables of local thickness (h1-h6) initially set to 0.35 m. Self-weight and a distributed wind load perpendicular to the inner surface is accounted for. Highly accurate surfaces are achieved penalizing maximum vertical displacements in the analysis.

The numerical model set-up in ANSYS software consists of 8880 quadrilateral plane stress elements (plane 82) with quadratic shape functions in a regular mesh. The elements thickness is constant for all elements (0.20 m) [5]. Consequential, the volume amounts to 0.35 m³. The total strain energy Π follows from Eq. 2 by integration of transposed elemental stresses σ and strains ε over the total volume V and gives 2.23 Nm.

$$\Pi=\frac{1}{2}\int_V \sigma^T\varepsilon\, dV \tag{2}$$

Twice the strain energy is equivalent to structural compliance, the inverted stiffness. Its physical interpretation is hence straightforward. Strain energy is obviously anti-proportional to structural stiffness. If the stiffness decreases, the strain energy rises and vice versa.

3 CROSS SECTIONAL OPTIMIZATION

The optimization process is split into five independent but subsequent steps reducing allowable vertical displacements from initially 9 to 5 mm in the end. In all steps the objective is to maximize the volume reduction by means of minimal local thicknesses (h1-h6). This is mathematically equivalent with finding the minimum structural compliance that grants the pre-scribed displacements. In general two optimization techniques are combined. At first, shape optimization fixes the outer contour of the parabolic trough that serves as the design space in subsequent topology optimization employing artificial material densities. The latter one then identifies domains where material is necessary for stiffness and others where hollow bodies reduce the total weight. Thereby, the output of shape optimization is simultaneously the input of topology optimization. To gain insight in the solution process of shape optimization by ANSYS two consecutive methods, zero-order and first-order-method are combined. They deliver the progress of the objective function and the design variables continuously.

3.1 Outer shape optimization

For the outer shape optimization, three different groups of variables have been defined. First group is the design variables x expressed by six heights (h1-h6) fixing the vertical distances between the radiation surface itself and its exterior end according to Fig. 2. These end points are connected one to another by a cubic spline function. At the very beginning equal heights (h_i=0.35) are stored in an initial vector but changed during iteration. Each iteration starts with the solution of the previous one by means of adapted values of height.
Second group are state variables g(x) used to restrict structural responses. They are formulated with respect to the design variables x and limited by upper (u) and lower (l) bounds (Eq. 3).

$$x = [x_1, x_2, \ldots, x_n]$$
$$x_{i,l} \leq x_i \leq x_{i,u} \qquad i = 1,2, \ldots n \tag{3}$$
$$g_{j,l} \leq g_j(x_i) \leq g_{j,u} \qquad j = 1,2, \ldots n$$

Restrictions are made concerning vertical displacements and concrete cracking that happens if stresses top the high-strength concrete's tensile strength. Generally, the higher the structural stiffness is, the lower deflections under constant loads are. Vertical displacements are reduced in five independent steps from initially 9 to finally 5 mm.

The last, third group comprises the objective function to be minimized. Here the volume of the trough subjected to self-weight and wind load shall be reduced to some extent. The wind load pressure according to Beaufort scale 6 is given with q = 0.18 kN/m² assuming an average pressure coefficient c_{pe} = 4 that integrates different load positions due to sun tracking and other but minor effects [2]. Tolerances of the three groups are defined separately. While the objective function's tolerance is set to 0.01 in ANSYS software, the design variables one is two times finer. For state variables a tolerance of 0.0002 is fixed.

Conceptually in this study, a two-step approach for shape optimization of the exterior shell contour is employed. However, the optimum determined this way is intermediate only and serves for subsequent optimization of topology discussed in section 3.2. Here, the focus is on shape optimization.

At first, a so called zero-order-method that relies on the design values, the state variables and the objective function but not on their derivatives is employed. It approximates the objective function by linear or quadratic polynomials according to Eq. 4. The coefficients herein a_0, a_i and b_{ij}, are obtained from regression employing weighted least squares to account for the restrictions set. Acc. to [5] the initially constrained optimization problem is transferred to an explicitly unconstrained one incorporating penalty terms for both, state variables and objective function.

$$f = a_0 + \sum_{i}^{n} a_i x_i \sum_{i}^{n} \sum_{j}^{n} b_{ij} x_i x_j \tag{4}$$

Next is to improve the approximation obtained above by a first-order-method employing derivatives. Here, the derivatives of the objective function are evaluated and stored in a gradient vector. In general, the method is known to be superior to the zero-order-approach since it finds local and global optima more accurate due to steepest descent and conjugate line-search techniques [5, 7]. However, this advantage comes along with a disadvantage. Obeying the total solution process, the method reduces the number of general iterations needed to converge at minimum but also requires a greater number of sub-iterations in intermediate loops. This condenses in higher time-demands for a global iteration but a smaller amount of iterations

compared to the zero-order-method. Additionally, it is possible to use zero-order-solutions obtained before as input for further optimization with the first-order-approach.

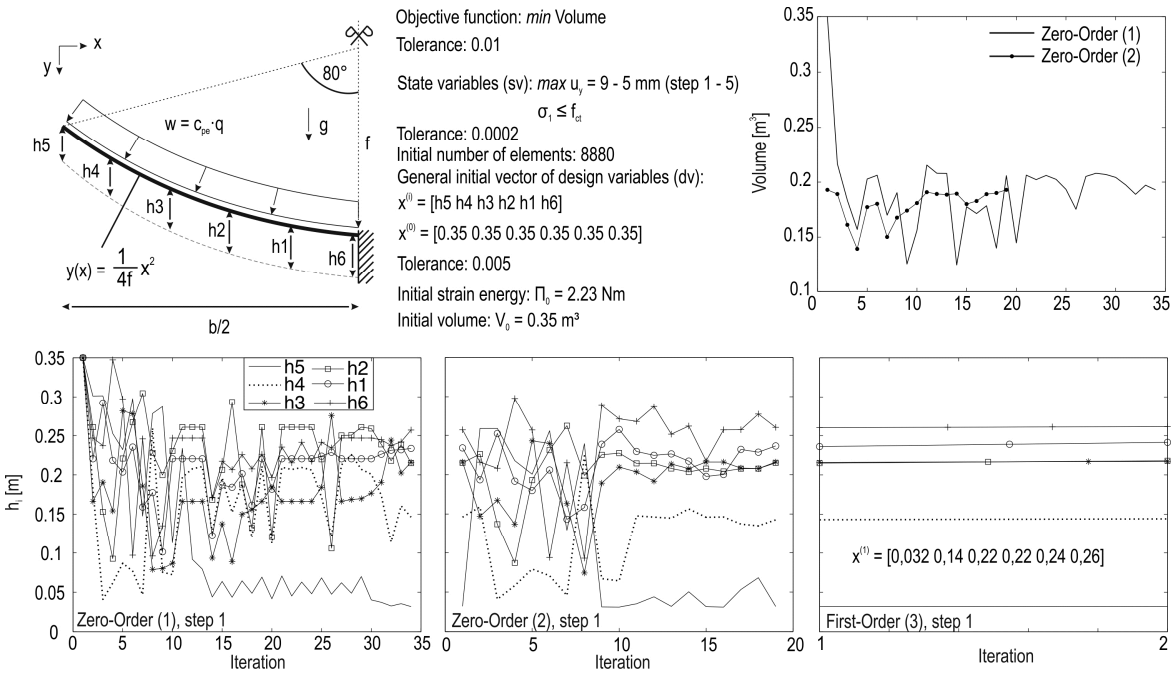

Figure 2: Cantilever beam as reduced cross sectional mechanical model (top left), general variables (top middle), objective function (top right) and design optimization progress for step 1 exemplarily (bottom).

Exemplarily the progress of shape optimization for limited vertical deflections (9 mm, step 1) employing the two consecutive methods discussed above is shown in Figure 2. At bottom three diagrams show the progress of the design variables during optimization. Six curves track the vertical heights (h1-h6) of the trough. While the first two diagrams were obtained from the zero-order-approach using approximation, the last one follows from the enhanced, derivative-based first-order-method. After 34 iterations, contained in the first graph, converging design variables could hardly be identified. Hence, another 17 iterations were performed. Thereafter all design variables have nearly converged. Physical interpretation is as follows: The closer the variable's location to the center, the higher its thickness. The final contour is crescent-shaped as shown in Fig. 4. Two more iterations by the enhanced method leave these results unchanged. However, the convergence rate of the latter shows significantly improved. Additionally, the objective function's progress in course of optimization is tracked in the upper-right graph of Fig. 2.

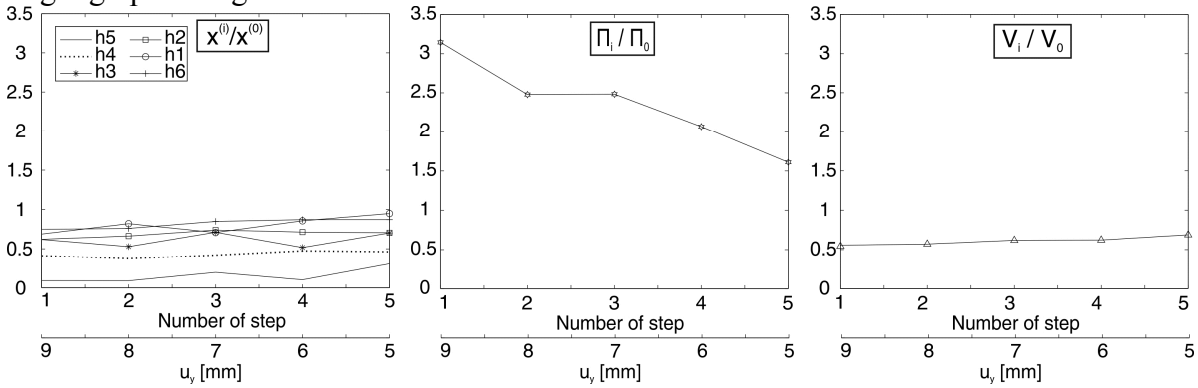

Figure 3: Design variables (h_i), stiffness indicator (strain energy Π_i) and objective function (volume V_i) related to their initial values for step 1-5.

Figure 3 shows the variation of the solution by means of three newly developed dimensionless indicators with step-wise intensified restriction of maximal deflection. On the horizontal axes step number and pre-scribed maximum deflection in mm is plotted, whereas the y-axes show the dimensionless indicators, e.g. design vector x, total strain energy Π and volume V. In general, the indicators relate current to the initial values and reveal global tendencies meanwhile the restriction of deflection is tightened. As expected the volume V as well as the design variables h_i show moderate increases, while the strain energy Π shows a steep descent. This sensitivity qualifies the strain energy as a perfect monitoring variable in structural optimization.

3.2 Topological optimization for identifying hollow shapes

By contrast to shape optimization, the design space in topology optimization is (already) fixed. Here, design variables (η_i) are internal pseudo-densities of finite elements [5, 6]. Thus a finite element mesh, a discretization of the design space, is a prerequisite for this method. Here, the same mesh introduced before has been used. For every element the pseudo-density lies between its limits of zero and one. Intermediate values are theoretically allowed but should be avoided. Physical meaning of a zero density is that belonging elements might be removed in terms of structural stiffness, whereas ones mark the opposite. Of course, the density value depends on boundary conditions and load patterns applied on the mesh but interestingly not on the size of loads. Defining both, loads and boundary conditions, on a mesh leads to a distribution of material according to the inner flux of forces. Besides these two, obviously, the number of elements of the discretization chosen strongly influences the results. Aside the material itself is of minor interest. In practical application it is mostly assumed linear elastic, e.g. defined by Young's modulus and Poisson's ratio. A final driving parameter of the results is the mass reduction factor beta according to Eq. 5.

$$m_{red} = (1-\beta)m_0$$
$$m_0 = \textit{initial mass},\ m_{red} = \textit{reduced mass} \tag{5}$$

It relates initial and final mass, thereby defining the extent of mass reduction allowed for in optimization. A typical strategy for topological optimization is to adapt the optimality-criteria (OC) algorithm. It minimizes the structural compliance, the inverse of structural stiffness, which equals twice the strain energy according to Eq. 2. Thereby, the mass reduction factor beta is fixed as a constraint [5, 6]. Consequently, the convergence of results must be checked to ensure optimality.

For this study, the situation is different. Since the structural stiffness of the concrete trough has already been determined by shape optimization before, the ideal mass reduction factor beta remains to be searched for. Sequential Convex Programming (SCP) is known to be advantageous for this purpose [7, 8, 9]. Figure 4 contains first results of structural optimization. The upper cross-section of the parabolic trough achieves a maximum volume reduction with respect to the here allowed compliance in a range from 7 to 8. Although both parameters - structural compliance and mass reduction factor beta - have converged obviously the material distribution lacks plausibility in parts of the structure. For comparison the compliance for the solid case (about 7.25 Nm) is added to the plot of compliances. It is lower than the one obtained by structural optimization and meets the expectation since the volume has been significantly decreased. Nevertheless, at center, close to the symmetry axis, clear substructures by means of struts and hollow domains, can be identified. Here the wall thickness is low as expected due to the stress limitations set. Aside, at the very end of the structure no material seems to be needed which is unacceptable. A quick workaround excludes these parts from the

optimization not allowing for material reduction at all. The remaining design space is again optimized and results in a more plausible material distribution along the whole structure, which is still subject of current investigations to gain robust hollow structures with maximum material mass reduction factors.

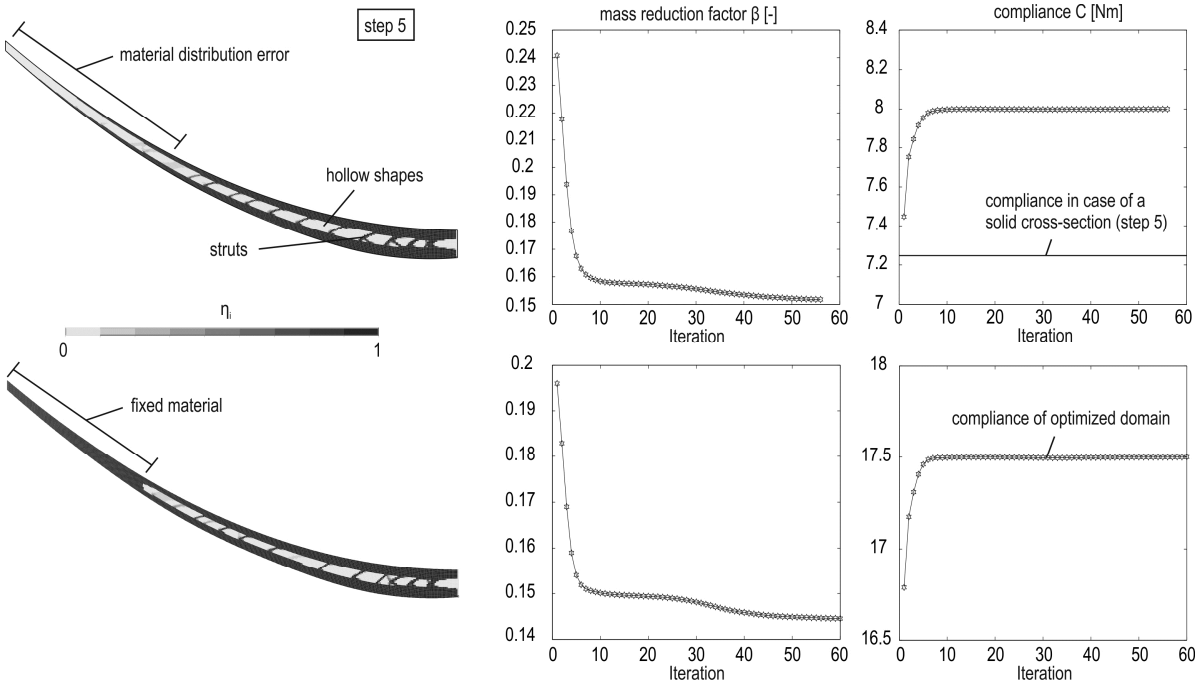

Figure 4: Material distribution (left), reduction factor β (middle) and maximum compliance (right) for initial (top) and reduced design space (bottom) of step 5.

4 CONCLUSIONS AND OUTLOOK

Large-scale parabolic troughs made from high-strength concrete have a high-potential being competitive on market. They can be cost efficient since serial production is a common concrete technology. Therefore, an essential prerequisite is an optimally balanced relation of stiffness and weight, to minimize material costs in construction and maximize bearing capacities subjected to a variety of different load cases expected during operation. In combination of two promising structural optimization methods a true-to scale prototype trough structure is set up and numerically analyzed in detail. Employing shape-optimization techniques in ANSYS software its outer contours are optimized with respect to concrete volume and the flux of inner forces. Meanwhile it also serves as the design space in a subsequent optimization step by means of topology optimization. Here, the solid inner concrete matrix is dissolved in distinct struts and hollow bodies leading to mass reductions about 15 % thereby fulfilling tight deflection limits of few millimeters. All intermediate solution steps and final results allow to be checked for adequacy and plausibility. A newly developed dimensionless progress indicator of the holistic optimization process identifies the total strain energy as the most sensitive parameter which is thus recommended for monitoring.

Remaining tasks for the future are the extrapolation of the hollow cross-section derived from structural optimization in longitudinal direction as well as the experimental verification by means of large-scale trough structures made of high-strength concrete including its smaller sub-structures in view of bearing capacities and structural stability.

5 ACKNOWLEDGEMENT

The authors thank the German Research Foundation (DFG) for the financial support of this project, which is part of the "Concrete Light" DFG priority program SPP 1542.

REFERENCES

[1] P. Forman, S. Müller, M.A. Ahrens, J. Schnell, P. Mark, R. Höffer, K. Hennecke, J. Krüger, Light concrete shells for parabolic trough collectors – conceptual design, prototype and proof of accuracy. *Solar Energy, Volume 111*, p. 364-377, 2015.

[2] S. Müller, P. Forman, J. Schnell, P. Mark, Leichte Schalen aus hochfestem Beton als Parabolrinnen solarthermischer Kraftwerke. *Beton- und Stahlbetonbau*, Ernst & Sohn Verlag, Volume 108, Issue 11, p. 752-762, 2013.

[3] P. Forman, S. Müller, Shape-optimised parabolic trough collectors made of micro reinforced ultra-high performance concrete. *9th fib International PhD Symposium in Civil Engineering,* Karlsruhe Institute of Technology (KIT), 22-25 July, Germany, 2012.

[4] P. Forman, S. Müller, Verformungsoptimierte Parabolrinnenkollektorschalen aus hochfestem Beton. *Tagungsband des 54. Forschungskolloquiums des Deutschen Ausschusses für Stahlbeton (DAfStb)*, Bochum, 2013.

[5] ANSYS® - *Handbook, Theory reference for the mechanical APDL and mechanical applications*. Release 12.1, U.S.A, 2009.

[6] M.P Bendsøe, O. Sigmund, *Topology Optimization – Theory, Methods and Application.* Springer Verlag, Berlin, 2003.

[7] L. Harzheim, *Strukturoptimierung – Grundlagen und Anwendung*. Europa Lehrmittel Verlag, 2. Auflage, Mainz, 2014.

[8] T. Putke, P. Mark, Fachwerkmodellbildung mit topologischen Optimierungsverfahren. *Beton- und Spannbetonbau*, Ernst & Sohn Verlag, Volume 109, Issue 9, p. 618-627 2014.

[9] Q. Ni, Ch. Zillober, K. Schittkowski, Sequential convex programming methods for solving topology optimization problems: implementation and computational results. *Journal of Computational Mathematics*, Volume 23, Issue 5, 2005.